Magnesium Technology 2011
Edited by: Wim H. Sillekens, Sean R. Agnew, Neale R. Neelameggham, and Suveen N. Mathaudhu
TMS (The Minerals, Metals & Materials Society), 2011

MICROSTRUCTURE, PHASE EVOLUTION AND PRECIPITATION STRENGTHENING OF Mg-3.1Nd-0.45Zr-0.25Zn ALLOY

G. Atiya, M. Bamberger, A. Katsman

Department of Materials Engineering, Technion, Haifa 32000, Israel

Keywords: Mg-Nd-Zn-Zr alloys, precipitation sequence, crystallographic structure, orientation relationship, hardening

Abstract

The microstructure of the Mg-3.1Nd-0.45Zr-0.25Zn (wt.%) alloy has been investigated after solution treatment at 540^{0}C for 24hr, followed by isothermal aging at 175^{0}C up to 32 days. Various electron microscopy techniques, like EDX mapping and TEM with SAED, have been used to characterize the phase composition and orientation relationships between different phases. After solution treatment, the BCT $(Mg_{1-x}Zn_x)_{12}Nd$ phase present in the as-cast alloy dissolved, and small tetragonal Zn_2Zr_3 rod-like particles precipitated in the α-Mg grain interiors. Zn_2Zr_3 particles are elongated along [001] direction, have an orientation relationship with the Mg matrix $[-2110](0001)_{Mg} \| [001](110)_{Zn2Zr3}$ and appear to be stable in the Mg matrix. Precipitation during isothermal aging involves the formation of metastable phases $\beta''(Mg_3Nd)_{HCP}$ (DO_{19} structure) and $\beta'(Mg_3Nd)_{FCC}$ (DO_3 structure). The β'' precipitates formed during the first 8 days of aging have a plate shape and are fully coherent with the Mg matrix, with the orientation relationship $[-2110](0001)_{Mg} \| [-2110](0001)_{\beta''}$ and $[-1100]_{Mg} \| [-1100]_{\beta''}$. The Zn_2Zr_3 rods serve as additional nucleation sites for precipitation during aging. The heterogeneous nucleation occurs in two ways: precipitates nucleate on the basal planes and on the side planes of the Zn_2Zr_3 rods. After 8 days of aging, these precipitates were identified as β'. During the 16÷32 days of aging, β'' precipitates in the grain interior transform into β' precipitates with an FCC structure. The β' precipitates are semi-coherent ith the Mg matrix and have the following orientation relationship: $[0001](2\text{-}1\text{-}10)_{Mg} \parallel [101](11\text{-}1)_{\beta'}$ and $[-1100]_{Mg} \| [-112]_{\beta'}$. In the late stage of aging, the β' precipitates transform into a stable incoherent β $(Mg,Zn)_{12}Nd$ phase. The growth, coarsening and phase transformations were followed by microhardness tests.

1. Introduction

Magnesium alloys containing rare earth (RE) elements have received extensive attention in recent years due to their excellent mechanical properties, especially high temperature creep resistance, light weight and good die-castability [1-5]. Mg alloys containing RE elements are age hardenable and the thin plate-like precipitates that are uniformly dispersed in the matrix are probably attributed to the mechanical properties and creep resistance. Small additions of Zn to Mg-Nd alloy systems would enhance the hardening ability. In addition, most Mg-RE alloys usually contain 0.4-0.6wt.% Zr as a grain refiner [1,6]. However, attempts to improve the hardness and the strength of these alloys are limited by lack of understanding of the structure, orientation and composition of precipitates and the influence of different alloying elements on the precipitation hardening. The research described in the present paper contributes to the investigation of the precipitation sequence in Mg-Nd based alloys in the presence of Zr and Zn. In addition, the crystallographic orientation of precipitates was studies in the grain interior and in the grain boundary regions.

2. Experimental

An alloy with a nominal composition of Mg-3.1Nd-0.45Zr-0.25Zn (wt.%) was prepared by the Dead Sea Magnesium Research Institute (MRI) . The samples were encapsulated in quartz tubes under 300mmHg Argon atmosphere and were solution treated (ST) for 24hr at 540°C followed by water quenching at 25°C. The treatment included heating to 225°C (heating rate of 10°C/hr), then heating to 540°C at a rate of 15°C/hr. Then the samples were aged in an oil bath at 175°C for up to 32 days. Phase analysis was carried out with X-ray diffractometer (XRD), the microstructure was examined using optical microscopy and FEI Scanning Electron Microscope (SEM), Quanta 200. EDS Analysis was conducted on TEM samples with a special specimen holder in order to increase the reliability and ensure that the photons are scattered from a specific analyzed region. Vickers Hardness testing was performed using 50gr load and holding time of 15sec. Precipitate microstructures were examined in FEI Tecnai G2 T20 S-Twin (TEM) and FEI Titan 80-300 FEG-S/TEM (HRTEM).

3. Results

3.1 As-cast Microstructure

The microstructure of the Mg-3.1Nd-0.45Zr-0.25Zn (wt. %) alloy in as-cast condition is shown in Figure 1. The microstructure consists of α-Mg matrix, eutectic compounds and Zr-rich particles. The average grain size is about 40μm. The eutectic compounds were analyzed by XRD analysis and TEM SAED pattern (Figure 2), and were identified as $Mg_{12}Nd$ with BCT structure (a=1.031nm c=0.593nm).

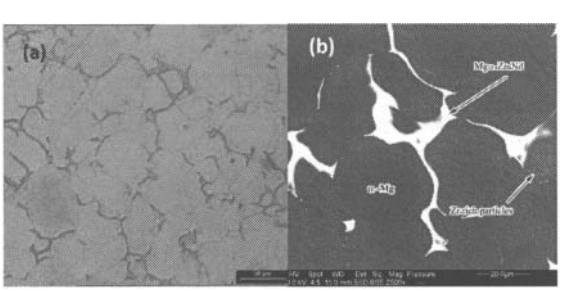

Figure 1. (a) Optical micrograph and (b) BSE SEM micrograph of Mg-3.1Nd-0.45Zr-0.25Zn showing as- cast microstructure.

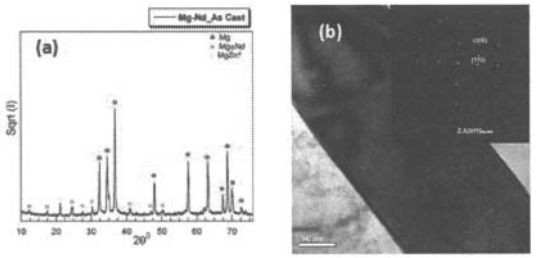

Figure 2. (a) XRD pattern of the Mg-3.1Nd-0.45Zr-0.25Zn as-cast alloy; (b) TEM BFI and corresponding SAED of the eutectic compound zone axis $[001]_{Mg_{12}Nd}$.

It was revealed by SEM EDS analysis performed on the TEM sample that Zn atoms substitute Mg atoms in the eutectic compound (~2.6at.%) as shown in Figure 3 and Table 1.

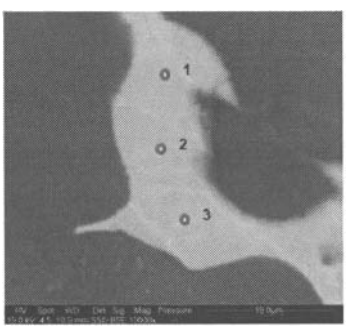

Figure 3. BSE SEM micrograph of the eutectic compound ir as-cast state.

Table 1. EDS element analysis conducted by SEM on the TEM sample

Spectrum	Mg(%at)	Zn(%at)	Nd(%at)
1	90.38	2.53	7.08
2	89.84	2.85	7.31
3	89.68	2.45	7.88
Mean	89.97	2.61	7.42
Std. deviation	0.37	0.21	0.41

3.2 ST Microstructures

As follows from XRD data (Figure 4), only α-Mg phase remains after solution treatment. However, detailed SEM and TEM investigations revealed residual eutectic compounds and Zn_2Zr_3 particles that are gathered in clusters (Figures 5, 6).

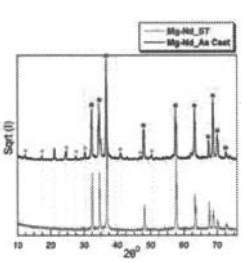

Figure 4. XRD pattern of investigated Mg-3.1Nd-0.45Zr-0.25Zn (wt.%) as cast and solution treated.

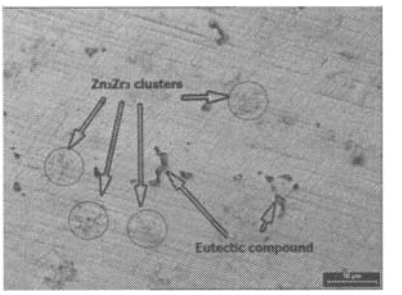

Figure 5. Solution treated microstructure showing Zn_2Zr_3 clusters and residual intermetallic phase at grain boundaries.

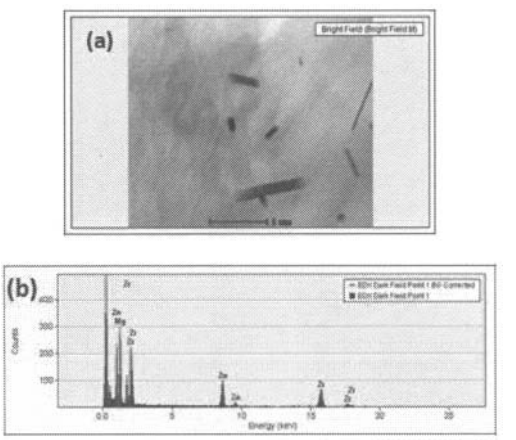

Figure 6. (a) STEM BF micrograph and (b) corresponding EDS spectrum of the Zn_2Zr_3 particle.

3.3 Precipitation Hardening During Aging

The aging of solution treated samples was performed at 175°C up to 32 days. The microhardness increases and reaches the maximum value of about 80HV after 8 days (Figure 7) and then decreases with the aging time.

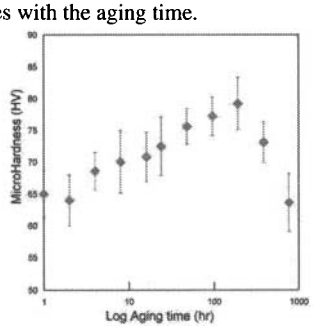

Figure 7. Microhardness as a function of time during isothermal aging at 175°C.

3.4 Phase Composition And Crystallographic Orientations of Precipitates After Aging

The peak aged (8 days aging) sample was investigated by TEM and HRTEM (Figures 8, 9). TEM micrograph and corresponding SAED from grain interior indicate the presence of metastable $\beta''(Mg_3Nd)_{HCP}$ (DO_{19} structure) precipitates. The precipitates have a plate shape and are fully

coherent with the Mg matrix, with the orientation relationship (OR) $[-2110](0001)_{Mg} \| [-2110](0001)_{\beta''}$ and $[-1010](-12-10)_{Mg} \| [-1010](-12-10)_{\beta''}$.
HRTEM image along $[-1010]_{Mg}$ zone axis (Figure 9) reveals β" plate precipitate that is fully coherent with the Mg matrix.

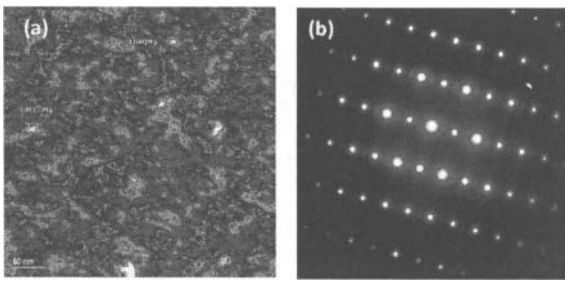

Figure 8. (a) BF TEM micrograph of β" precipitates in the Mg matrix after 8 days of aging and (b) corresponding SAED $[-2110](0001)_{Mg} \| [-2110](0001)_{\beta''}$.

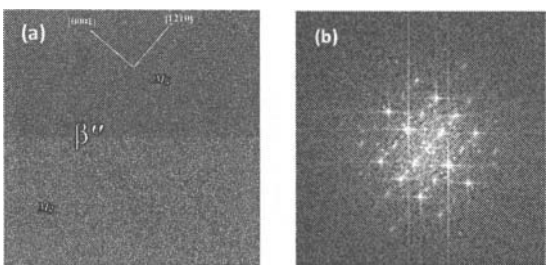

Figure 9. (a) HRTEM micrograph of β" precipitates in the Mg matrix and (b) corresponding Fast Fourier Transform (FFT) $[-1010](-12-10)_{Mg} \| [-1010](-12-10)_{\beta''}$.

The Zn_2Zr_3 rods, distributed in the grain interior, serve as additional nucleation sites for precipitates. The tetragonal Zn_2Zr_3 particles ($P4_2/mnm$: a=0.768nm and c=0.699nm) which seem to have a near octagon cross-section (Figure 10), are elongated along [001] direction, have an orientation relationship with the Mg matrix $[-2110](0001)_{Mg} \| [001](110)_{Zn2Zr3}$ and appear to be stable in the Mg matrix.

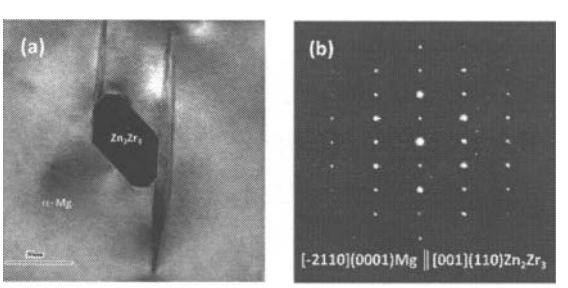

Figure 10. (a) BF TEM micrograph of Zn_2Zr_3 rod particle elongated to [001] direction; (b) corresponding SAED of Mg and Zn_2Zr_3 with the OR $[-2110](0001)_{Mg} \| [001](110)_{Zn2Zr3}$.

Nd-rich plate-like precipitates nucleate on the side and basal planes of the Zn_2Zr_3 as identified by EDS mounted on the TEM (Figures 11, 12). It is accompanied by the formation of precipitation free zones (PFZs) near Zn_2Zr_3 rod particles.

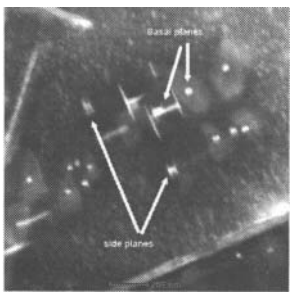

Figure 11. DF STEM micrograph of Zn_2Zr_3 particles with Nd-rich plate-like precipitates on their basal and side planes.

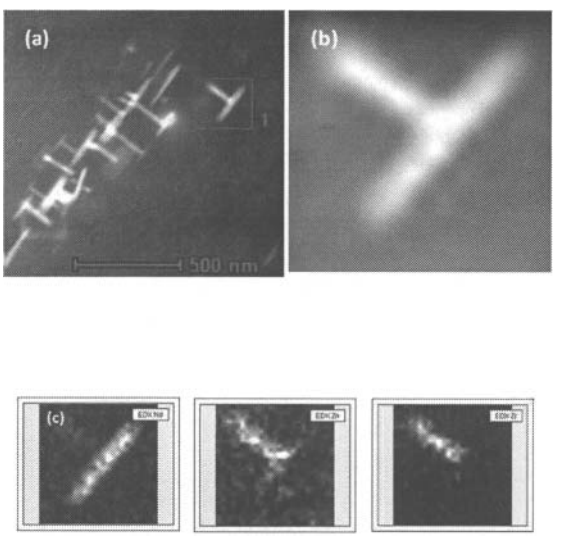

Figure 12. (a) DF STEM micrograph of Zn_2Zr_3 with Nd-rich plates on the basal and side planes; (b) EDS mapping area; (c) mapping of elements by EDS.

These plate-like precipitates were identified by SAED as $\beta'(Mg_3Nd)_{FCC}$ (DO_3 structure) with the following OR $[0001](2\text{-}1\text{-}10)_{Mg} \| [101](11\text{-}1)_{\beta'}$ (Figure 13).

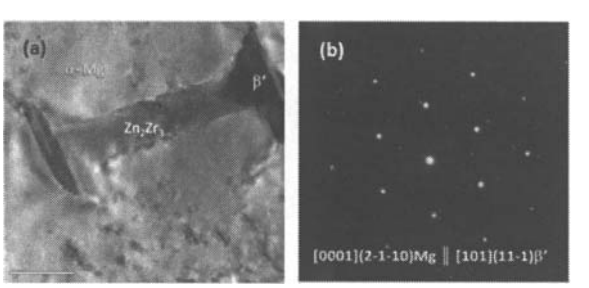

Figure 13. TEM micrograph and corresponding SAED of β' precipitate nucleated on Zn_2Zr_3 rod particle.

The β'-phase was also found in the grain boundary regions. Figure 14 provides TEM micrograph and corresponding SAED from the grain boundary region. A small number of

large precipitates (few hundreds of nm in size) and a high density of fine β'-precipitates were observed.

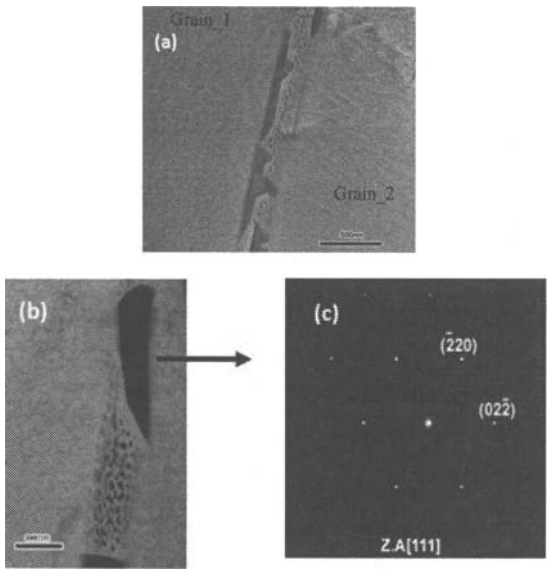

Figure 14. (a) TEM micrograph of grain boundary region; (b) BF TEM micrograph of β' precipitate in the grain boundary region; (c) corresponding SAED from large $\beta'(Mg_3Nd)_{FCC}$ ZA [111].

It was proved by HRTEM analysis (Figure 15) that the small precipitates (5-50nm in size) are β' as well.

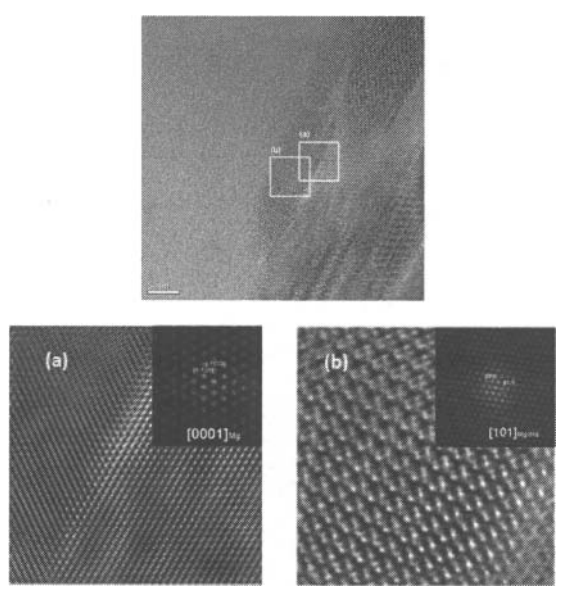

Figure 15. HRTEM micrograph of small precipitates in the grain boundary region (a) filtered HRTEM image and corresponding FFT of Mg matrix (b) filtered HRTEM image and corresponding FFT of β' precipitate

After 32 days of aging, it was found that β" phase transforms into β' in the grain interior and β' precipitates transform into β in the grain boundary regions.

4. Discussion

Precipitation during isothermal aging involves the formation of metastable phases $\beta''(Mg_3Nd)_{hcp}$ (DO_{19} structure) and $\beta'(Mg_3Nd)_{fcc}$ (DO_3 structure), and this is consistent with the precipitation sequence of [1,7]:

$$ssss(Mg) \rightarrow GP\ Zones \rightarrow \beta'' \rightarrow \beta' \rightarrow \beta.$$

Among these precipitates, the coherent β" and semicoherent β' are the primary strengthening phases while the β phase exists usually in an overaged condition and exhibits a lower strengthening effect. Zirconium-rich cores are often present in the center of the grains, when zirconium is used as a grain refiner. In addition, in an alloy containing Zn, Zn_2Zr_3 phase forms after solution treatment [8]. As found in the present research, the Zn_2Zr_3 rods are elongated along $[001]_{Zn2Zr3}$ direction and has OR with the Mg matrix $[-2110](0001)_{Mg} \| [001](110)_{Zn2Zr3}$ (Figure 10) in correspondence with the results of Gao et al. [9]. It means that Zn_2Zr_3 rods grow parallel to the basal planes of the Mg matrix. Therefore it probably has minor influence on the alloy hardness. However, they serve as additional nucleation sites for β" and β' plate-like precipitates, which may be perpendicular or parallel to the Mg basal planes (Figures. 11, 12). They may substantially influence basal and non-basal dislocation movement resulting in additional hardening. The β' plates adjacent to Zn_2Zr_3 are much bigger than β" plates distributed in the α-Mg matrix. It can be explained by their earlier nucleation followed by coarsening. The formation of PFZs around β'-precipitates confirms the coarsening process. At the peak aged condition, the β' precipitates are formed in the grain boundary regions, whereas β" are formed in the grain interior, as discussed above (Figures. 8, 14). Faster diffusion of Nd along grain boundaries may explain earlier transformation of β" into β' in the grain boundary region. High density of fine β' and a small number of large β' precipitates illustrate the coarsening process at the grain boundary area accompanied by formation of PFZs.

5. Conclusion

Eutectic phase $(Mg_{1-x}Zn_x)_{12}Nd$ with BCT crystal structure dissolves during ST, and small tetragonal Zn_2Zr_3 rod-like particles precipitate in the α-Mg matrix and near grain boundaries. Zn_2Zr_3 rod-like particles were found elongated along $[001]_{Zn2Zr3}$ direction and has the following orientation relationship: $[-2110](0001)_{Mg}//[001](110)_{Zn2Zr3}$. The Zn_2Zr_3 rods serve as additional nucleation sites for precipitation during aging. After 8 days of aging at 175°C, plate-like precipitates of a metastable β" $(Mg_3Nd)_{HCP}$ phase with DO_{19} structure formed in the grain interior. The β" precipitates are fully coherent with the Mg matrix with the OR $[-2110](0001)_{Mg} \| [-2110](0001)_{\beta''}$. Plate-like precipitates of $\beta'(Mg_3Nd)_{FCC}$ (DO_3 structure) phase were found in the grain boundary regions and on the side and basal planes of Zn_2Zr_3 rod particles. The β' precipitates are semi-coherent with the Mg matrix with the OR $[0001](2\text{-}1\text{-}10)_{Mg} \| [101](11\text{-}1)_{\beta'}$. During the 16÷32 days of aging, β"- precipitates in the grain interior transform into the β' precipitates with an FCC structure. In the late stage of aging, the β'-precipitates transform into a stable incoherent β $(Mg,Zn)_{12}Nd$ phase.

References

1. Pike, T. J.; Noble, B. *Journal of the Less Common Metals* **1973,** 30, (1), 63-74.
2. Nie, J. F.; Muddle, B. C. *Acta Materialia* **2000,** 48, (8), 1691-1703.
3. Zheng, K. Y.; Dong, J.; Zeng, X. Q.; Ding, W. J. *materials Science and Engineering: A* **2008,** 489, (1-2), 44-54.
4. Penghuai, F.; Liming, P.; Haiyan, J.; Lan, M.; Chunquan, Z. *Materials Science and Engineering: A* **2008,** 496, (1-2), 177-188.
5. Apps, P. J.; Karimzadeh, H.; King, J. F.; Lorimer, G. W. *Scripta Materialia* **2003,** 48, 8), 1023-1028.
6. Wilson, R.; Bettles, C. J.; Muddle, B. C.; Nie, J. F. In *Precipitation hardening in Mg-3 wt%Nd(-Zn) casting alloys*, Materials Science Forum, 2003; 2003; pp 267-272.
7. Rokhlin, L. L., *Magnesium alloys containing rare earth metals*. 2003; Vol. 3.
8. Fu, P.; Peng, L.; Jiang, H.; Zhai, C.; Gao, X.; Nie, J. F. In *Zr-containing precipitates in Mg-3wt%Nd-0.2wt%Zn-0.4wt%Zr alloy during solutionTreatment at 540_°C*, Materials Science Forum, 2007; 2007; pp 97-100.
9. Gao, X.; Muddle, B. C.; Nie, J. F., Transmission electron microscopy of Zr€"Zn precipitate rods in magnesium alloys containing Zr and Zn. In Taylor & Francis: 2009; Vol. 89, pp 33 - 43.